

<https://helda.helsinki.fi>

Structural properties of protective diamond-like-carbon thin films grown on multilayer graphene

Liu, Jian

2019-12-18

Liu , J , Muinos , H V , Nordlund , K & Djurabekova , F 2019 , ' Structural properties of protective diamond-like-carbon thin films grown on multilayer graphene ' , Journal of Physics. Condensed Matter , vol. 31 , no. 50 , 505703 . <https://doi.org/10.1088/1361-648X/ab4094>

<http://hdl.handle.net/10138/308762>

<https://doi.org/10.1088/1361-648X/ab4094>

cc_by_nd

acceptedVersion

Downloaded from Helda, University of Helsinki institutional repository.

This is an electronic reprint of the original article.

This reprint may differ from the original in pagination and typographic detail.

Please cite the original version.

Structural properties of protective diamond-like-carbon thin films grown on multilayer graphene

Jian Liu^{a,b}, Henrique Vazquez Muinos^a, Kai Nordlund^a, Flyura Djurabekova^{a,*}

^a*Helsinki Institute of Physics and Department of Physics, University of Helsinki, POB 43, 00014, Helsinki, Finland*

^b*Department of Nuclear Science and Engineering, Nanjing University of Aeronautics and Astronautics, Nanjing 210016, China*

Abstract

In spite of the versatility of electronic properties of graphene, its fragility and low resistance to damage and external deformations reduce the practical value of this material for many applications. Coating of graphene with a thin layer of hard amorphous carbon is considered as a viable solution to protect the 2D material against accidental scratches and other external damaging impacts. In this study, we investigate the relationship between the deposition condition and quality of diamond-like-carbon (DLC) on top of multilayer graphene by means of molecular dynamics simulations. Deposition of carbon atoms with 70 eV incident energy at 100 K resulted in the highest content of sp^3 -bonded C atoms that amounted to 15.9%. An increase of the number of dangling bonds at the interface between the top graphene layer and the DLC film indicates that increase of the incident energy reduces the adhesion quality of DLC thin film on graphene. Analysis of radial distribution function indicates that sp^3 hybridized carbon atoms tend to grow near already existing sp^3 -atoms. This explains why the quality of the DLC structures grown on graphene have generally a lower content of sp^3 C atoms compared to those grown directly on diamond. Ring analysis further shows that a DLC structure grown on the sp^2 -rich structures like graphene contains a higher fraction of disordered ring structures.

Keywords: Diamond-like-carbon, Multilayer graphene, Molecular dynamics, Carbon atoms deposition

*e-mail: flyura.djurabekova@helsinki.fi

1. Introduction

With the rapid development of nanoscience and nanotechnology, carbon nanomaterials, such as fullerenes [1], carbon nanotubes [2] and graphene [3], have gained much attention. Many scientific efforts are dedicated to study the properties and investigate potential applications of these carbon nanomaterials. Amongst these, graphene is the most promising stable 2D material. Moreover, its unique properties such as mechanical resistance [4], electrical [5] and thermal [6] conductivity etc, compared to conventional macro-materials make graphene a promising material in various applications such as gas sensing [7], water purification, [8] and touch screens [9] in the future. However, the attractive properties of graphene can alter severely due to mechanical wearing, scratching [10], or parasitic irradiation in space applications [11, 12]. The damage of graphene in daily used graphene-based appliances and equipments, will surely shorten the serving time of the latter. Thus, it is of great importance to find a compatible durable coating to protect graphene and enhance its resistant ability against external damage.

Diamond-like-carbon (DLC), is reported to be an ideal protective material for nanostructures and is able to enhance mechanical strength of nanomaterials [13–15]. DLC exhibits many desirable properties, such as ultra-high hardness and elastic moduli [16], low friction coefficient [17], transparency in the IR wavelength band [18] and chemical inertness [19]. Moreover, it is highly compatible with graphene structure. DLC coating is already widely used in many applications, e.g. as an antireflection layer for IR optic devices [20] or a protection layer for magnetic storage components [21] and an anticorrosion layer for biocompatible materials [22]. It will be utilized extensively even more in various fields like electronics, aviation, aerospace etc. [23–25]. In addition, some research has been carried out to analyze the protective properties of DLC films coating nanostructure both experimentally [15, 26–31] and by simulations [32–34]. In particular, Ren *et al.* [35] analyzed the effect of experimental conditions such as the combination of incident energy and ambient temperature on the quality of growing DLC film directly on diamond and on nanotubes placed on a diamond substrate, showing that a stable DLC can grow above a nanotube structure. The above-mentioned research shows that it is feasible to grow a DLC protective layer on top of carbon nanostructures. However, it is not entirely clear what defines the

quality of the grown DLC films, in order to predict their protective properties. Unfortunately there are only few reports about the quality of DLC deposited on top of graphene in different conditions. DLC, which is a variety of amorphous carbon, shows diverse properties with a different ratio of sp^2 and sp^3 hybridization [36]. It was seen that the higher sp^3 fraction the DLC has, the harder and denser it becomes [37]. Therefore, in the current paper we aim to find out how the deposition condition during the growth of thin films can define the quality of DLC above graphene, in order to enable the growth of high quality DLC protective layers.

Atomistic simulation methods are powerful tools to study mechanisms of atomic migration and collision, and eventually, the formation of the bonds within the materials. In this paper, we utilized classical molecular dynamics (MD) to simulate and study the process of carbon ion beam deposition with different incident energies at different temperatures on the top of multilayer graphene. Then, we analyzed the atomic structure, density and sp^3 fraction of grown DLC films in different conditions in order to reveal what inherent mechanisms lead to failure of growth of stable and dense DLC structures.

2. Simulation and analysis methods

Simulations of DLC deposition process shown in this paper were carried out with classical MD code PARCAS [38, 39]. In order to describe the interaction between carbon atoms, the empirical analytical bond-order Brenner-Beardmore potential [40–42] was applied. We used the extended low-end ($R=1.95$ Å) and high-end ($S=2.25$ Å) cutoff parameters, following Jäger and Albe’s work [43] to improve the description of formation of sp^3 -hybridization of carbon atoms. The extended cutoffs allowed depositing DLC with higher sp^3 fraction, which compares better to experimentally grown DLC films [35]. (COMMENT: Kai, could you write up this part with the potentials?) Unfortunately none of the classical potentials are able to predict correctly the formation of sp^3 bonded atoms [44], however, the selected potential with the extended cutoff can provide the understanding of comparative effect of DLC growth conditions. All the visualized simulation cells in this paper were obtained with the help of open visualization tool OVITO [45].

Figure 1 shows the schematic diagram of the initial multilayer graphene placed on top of the diamond substrate. For the sake of convenience, all sp^3 -hybridized C atoms are colored red in this and the following figures, while sp^2 -hybridized C atoms are colored blue. This structure was built up as

follows. The diamond substrate with the $\langle 111 \rangle$ surface normal and the size of $30 \times 30 \times 20$ Å included 3456 atoms. Six layers of graphene, 2304 atoms, were placed above the diamond substrate with the layer spacing of 3.35 Å (the interlayer distance in graphite), and the distance between diamond surface and bottom graphene was also 3.35 Å. To minimize the energy of multilayer graphene system, all the six layers of graphene were stacked in the A-B Bernal order. Third, periodic boundary condition was set in lateral (x and y) directions, leaving z -direction an open surface to deposit DLC.

We used the Berendsen [46] thermostat to control the temperature at the lateral borders within the 5 Å region and the two bottom layers of diamond atoms were fixed in order to dissipate heat and prevent the entire system from moving downwards during the continuous carbon ion beam irradiation. At last, incident carbon atoms were set 5 Å above the top layer of graphene with the velocity directed perpendicular to the graphene layers in the direction of the surface. The incident energies for the deposition process was varied between 50, 70, and 100 eV, in different sets of the subsequent deposition simulations. Before each carbon atom impact, a random cell shift in the xy plane was performed to ensure that carbon atoms would hit the whole graphene layer uniformly. Each ion impact was simulated for the total time of 10 ps to allow the generated heat to dissipate naturally at the boundaries of the simulation cell. As carbon atoms were arriving on graphene, the DLC film was gradually growing up and the initial incident position of depositing carbon atoms was also shifted up to ensure that there is always 5 Å distance to the highest z -coordinate of an atom in the cell of the current size to avoid extreme repulsive forces caused due to inappropriately short distances between newly appeared incident atom and already existed DLC. The ambient temperature was set as 100 K during the DLC film deposition. For each energy, around 8000 carbon impacts were carried out to obtain the desired volume of DLC for further analysis.

To evaluate the quality of the grown DLC film, we analyzed the sp^3 fraction, mass density, radial distribution function (RDF), and primitive rings in all the grown structures. We set the first cutoff length as 1.9 Å, as an average value between the first and the second peaks in the total RDF, respectively, see Figure 3. All the atoms with the three neighbours within the selected cutoff were considered as three-fold carbon atoms, or as the sp^2 hybridized ones, while four-fold atoms are counted as having sp^3 hybridization. Apart from the total RDF for all atoms, we also computed the RDF for only the sp^2 and the sp^3 hybridized atoms to deconvolute the total RDF and ana-

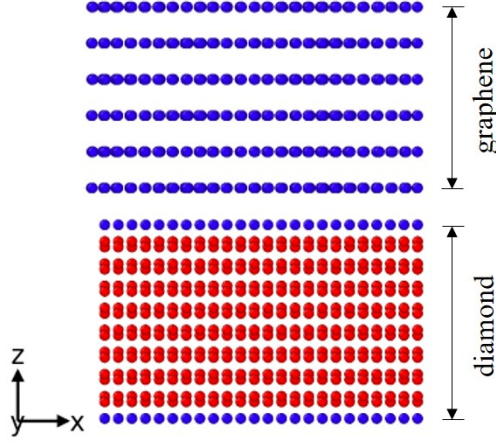


Figure 1: Schematic diagram of diamond and multilayer graphene model. Red atoms represent sp^3 hybridization while blue atoms stand for sp^2 hybridization.

110 lyze the short range order of both types of atoms in the grown DLC films.
 111 To inspect the total disorder degree, we also performed the primitive rings
 112 analysis [47]. In addition, the dangling bonds of carbon atoms located in
 113 the interface between graphene surface and bottom of the DLC were also
 114 analyzed to evaluate adhesion quality of the DLC film.

115 3. Results and discussion

116 3.1. sp^3 fraction and mass density

117 Figure 2 shows the distribution of the sp^3 fraction and mass density of
 118 the low-energy-ion deposited DLC film with the different incident energies
 119 along the z -axis (perpendicular to the surface) and corresponding simulation
 120 cells at 100 K and incident energies of 50, 70, and 100 eV, respectively. The
 121 four ticks to the right of the simulation cells are used to guide the eye to
 122 the location of the bottom and the top of the simulation cells, as well as of
 123 both interfaces (diamond-graphene and graphene-DLC). These four positions
 124 corresponds to four turning points in the relevant graphs, see Figure 2(a,c,e).
 125 In all these subfigures, the diamond and graphene regions are well visible
 126 since diamond has maximum density of 3.6 g/cm³ and consists of pure sp^3
 127 carbon atoms while graphene has minimum density of 1.8 g/cm³ and is made
 128 of pure sp^2 carbon atoms. As z -coordinate increases, the average density
 129 increases fluctuating around 2.7 g/cm³. At the same time, some increase in

130 the sp^3 fraction is also observed. This behavior of the mass density and sp^3
 131 fraction indicate the presence of the grown DLC film. We note here that the
 132 number of the sp^3 -hybridized atoms is slightly higher in the middle of the cell,
 133 further away from the interface and the open surface, where excess of the free
 134 volume can impede formation of the sp^3 -bonds. The stress exerted on sp^2
 135 carbon atoms by deposition of energetic carbon atoms and the continuously
 136 growing DLC film, the π C–C bond breaks converting into a σ C–C bond.
 137 This process results in formation of four σ covalent bonds corresponding to
 138 sp^3 hybridization instead of three σ and one π bonds corresponding to the
 139 sp^2 hybridization. On the other hand, the abundance of the sp^2 -hybridized
 140 carbon atoms in graphene, the first layer of the growing film (right above
 141 graphene layers) consists mainly of the same sp^2 carbon atoms, constituting
 142 the loose amorphous carbon structure at the bottom of the DLC film.

143 While analyzing the sp^3 fractions in the DLC grown structures with dif-
 144 ferent incident energies, we see that most sp^3 fraction forming in DLC films
 145 grown with 70 eV incident energies than other two energies. This indicates
 146 that there exists an optimal incident energy to form highest sp^3 fraction. On
 147 the other hand, the images in Figure 2 show that with increase of incident
 148 energy of deposited C atoms, fewer layers of the graphene remain intact.

149 Reduction of the number of graphene layers means that graphene is par-
 150 tially consumed by the grown DLC film and some of the sp^2 carbon atoms
 151 from the original graphene layers transformed in the sp^3 hybridized atoms.
 152 Hence, the average sp^3 fraction obtained in the cell grown at 100 K with the
 153 70 eV incident carbon ions is higher than that of 50 eV. Although higher de-
 154 position energy increases the conversion of the activated graphene sp^2 atoms
 155 to become part of the DLC film, it also means that the sp^2 -to- sp^3 conver-
 156 sion is promoted due to sufficient local stress generated by more energetic
 157 ions capable of penetrating deeper into the cell compared to those of 50 eV
 158 energy. This effect makes a notable difference only at low temperature like
 159 100 K since low temperature helps it stabilize the local concentration of the
 160 stress. Since sp^2 covalent C–C bonds are energetically more favorable [48],
 161 any temperature increase (also due to energetic ion impacts) in the disordered
 162 structure of amorphous carbon may reduce the local stress, causing sponta-
 163 neous transition of forming sp^3 C–C bonds into sp^2 C–C bonds, reducing
 164 overall the sp^3 fraction.

165 The mass density of the DLC films grown under different conditions along
 166 with the corresponding sp^3 content are listed in Table 1. We note that the
 167 simulation process of the film growth is time-consuming, this is why we report

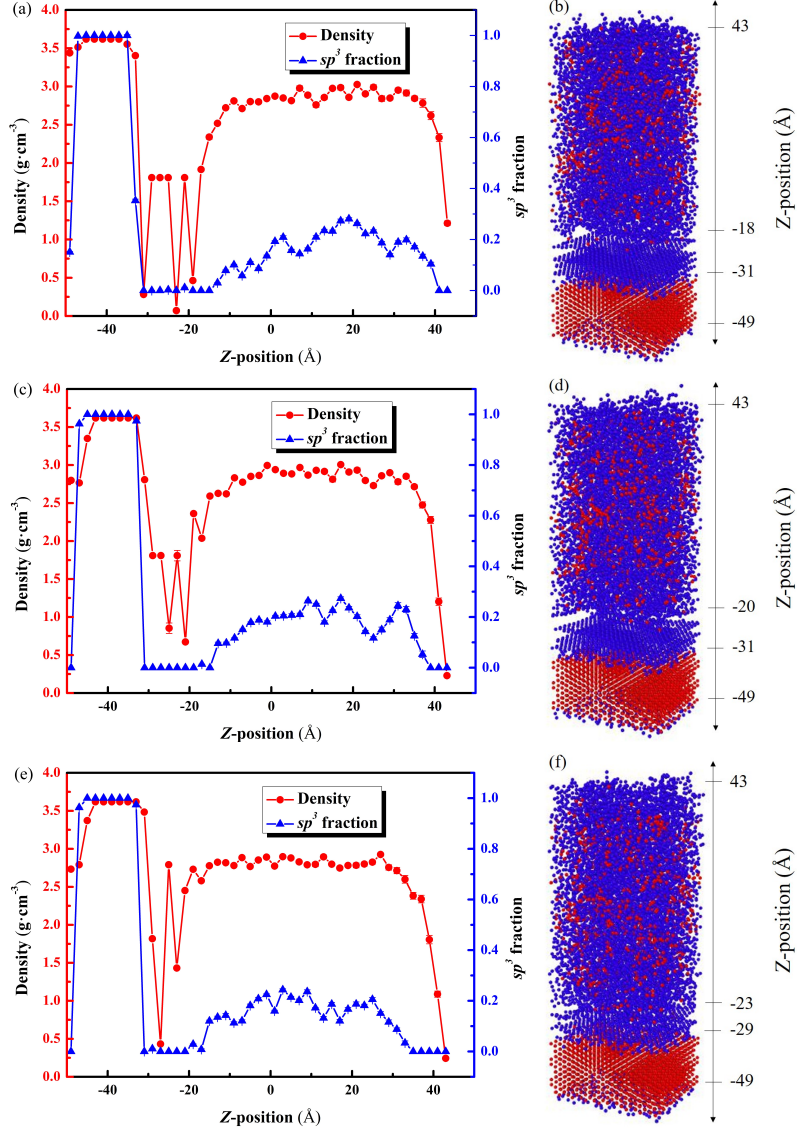


Figure 2: sp^3 fraction (right-hand y -axis) and mass density (left-hand y -axis) of the simulation cells as a function of z -coordinate with the incident energies of a): 50 eV; c): 70 eV; and f) 100 eV. The corresponding post-deposition simulation cells are shown in (b), (d), and (f), respectively. Red circles indicate the atoms with sp^3 -hybridized bonds and blue are the atoms with sp^2 ones. The error bars show the standard deviation in the analysis of all the atoms in the corresponding structure.

Table 1: Mass density (g/cm³) and sp^3 content (%) of DLC films deposited at different incident energies.

Energy (eV)	Mass density (g/cm ³)	sp^3 content (%)
50	2.728	14.9
70	2.766	15.9
100	2.704	13.8

here the results of analysis of a single structure for each energy, aiming mainly qualitative comparison of different deposition conditions. In Figure 2, where the error bars are the standard deviations from the mean value estimated either from the distribution or from the last frames of each of 10 last cascades (incident ion events). In this table, we see that the sp^3 fraction shows much stronger dependence on the incident energy than the average mass density of the grown DLC.

To investigate this effect further we plot now the radial distribution functions for two grown DLC structures with the highest and lowest content of sp^3 atoms to identify the difference in the short range order of all the carbon atoms within this structures. Figure 3 shows the radial distribution function grown with 70 and 100 eV, as well as deconvolution of the peak into the sp^2 and sp^3 components. We show all bonds within the high-end cutoff parameter 2.25 Å of the Brenner potential, which includes only the first nearest neighbors. We see that the expected value of the bond length in the entire structure that was grown at 100 K is around 1.49 ± 0.07 Å and is independent of incident energy. Hereafter the error bars indicate the standard deviation in the value of the bond length for all the atoms in the corresponding structure. For comparison, the bond lengths in graphene and diamond structures in the Brenner interatomic potential with the extended cutoffs used in the present study are 1.459 ± 0.048 Å and 1.545 ± 0.0001 Å, respectively. These values are close to those reported in the experiments, at least for the diamond structure it is known to be 1.54 Å [49]. The bond length in graphene can be estimated as a weighted average between two single bonds and one double bond ($a_{C=C} = 1.34$ Å [50]), which amounts to 1.47 Å.

When we analyze separately the expected values of the sp^2 - and sp^3 -bond lengths, we found them to be the same in both structures shown in Figure 3 and amounted to 1.46 ± 0.04 Å and 1.6 ± 0.09 Å, respectively. We see that the average bond length in the grown DLC structures for the sp^2 -bonded

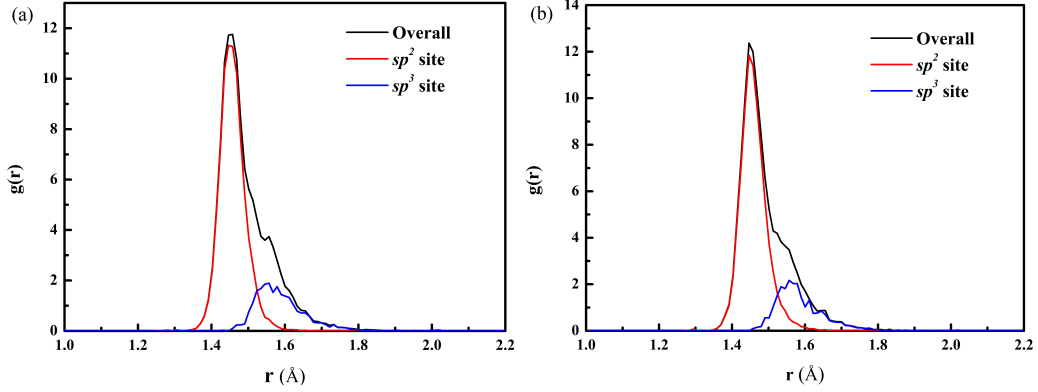


Figure 3: Radial distribution function $g(r)$ for DLC deposited at 100 K under incident energies of (a) 70 and (b) 100 eV, respectively. The contributions of sp^2 and sp^3 coordination are presented separately in red and blue color.

atoms is very close to that in ideal graphene, while the sp^3 -bonds are slightly stretched. Also there is some variation in the mean values of the sp^3 -bond lengths because of relatively small number of the atoms with such bonds, the amount of these atoms clearly affects the average bond length in the entire structure.

Overall, in both cases we observe much higher peak of the sp^2 -bonds compared to sp^3 ones as seen in Figure 3, even for the best structures with the highest density and highest sp^3 -content. As it was shown in [35], sp^3 carbon atoms tend to grow near the atoms which already are sp^3 -bonded as in diamond. Since we deposited the DLC film on top of graphene layers, the deposited atoms were landing next to the atoms with the sp^2 -bonding, forming the same sp^2 -bonds in more preferable manner. In other words, we observe the lack of formation of the sp^3 -bonded carbon atoms during the initial stage of film deposition, which is consistent with the observations in [35].

Although the bond length of the sp^2 -hybridized atoms is shorter, indeed they form only if there is sufficient free volume in the structure. It is also obvious in the values of the mass densities of the grown DLC structures: The higher the sp^3 content in the grown film, the higher its mass density is. In graphite, this inconsistency is explained by the large interlayer distance, while the interlayer distance in amorphous carbon is ill-defined. This is why we further analyze the average atomic volume in the DLC structures with the highest and the lowest sp^3 fraction. For this purpose we employ the

Table 2: Average atomic volume with the standard deviation calculated for the carbon atoms in the DLC films deposited at different temperatures and incident energies.

Energy (eV)	Average atomic volume (\AA^3)	
	sp^2 atoms	sp^3 atoms
50	7.53 ± 1.59	6.08 ± 0.65
70	7.44 ± 1.12	6.12 ± 0.66
100	7.58 ± 1.31	6.15 ± 0.61

Voronoi tessellation analysis available in OVITO software. According to this analysis, the average atomic volumes in multilayer graphene and diamond are $9.233 \pm 0.345 \text{ \AA}^3$ and $5.678 \pm 0.001 \text{ \AA}^3$, respectively.

In Table 2, we list the average atomic volume separately for sp^2 and sp^3 atoms in DLC films deposited at different incident energies at 100 K. We see that the average atomic volume is larger in the cells with the lowest content of sp^3 bonding, which explains the lower mass density. It is surprising that the atomic volume for the sp^3 -bonded atoms is very similar in all structures although it is slightly larger than in pure diamond. This indicates that the formed sp^3 atoms are stable and the bond stretching is mainly explained by the large amount of the sp^2 -bonded atoms, which occupy much larger volume per atom. The slightly smaller atomic volume for the sp^2 -bonded atoms are explained by densification during the impact.

3.2. Ring analysis

Different atomic volumes occupied by the sp^2 -bonded atoms indicates that there can be structural differences in the grown films. To investigate the nature of this differences, we performed the analysis of the primitive rings for quantitative investigation of the degree of long range disorder in the deposited DLC films. We chose the same structures as analyzed in Figure 2, namely the films grown at 100 K with all three incident energies. For this analysis we used the method described in Ref. [47], excluding the top 20 \AA of the DLC structure.

In Figure 4, we see that the three DLC structures grown at 100 K have similar distributions of the primitive rings. We see mainly the seven- to ten-member rings, although the number of the six-member rings is only slightly smaller than the larger rings. The five-member rings quite prominent in these structures as well. We see that the amount of the primitive rings with the large number members starts decreasing above 8-member rings in

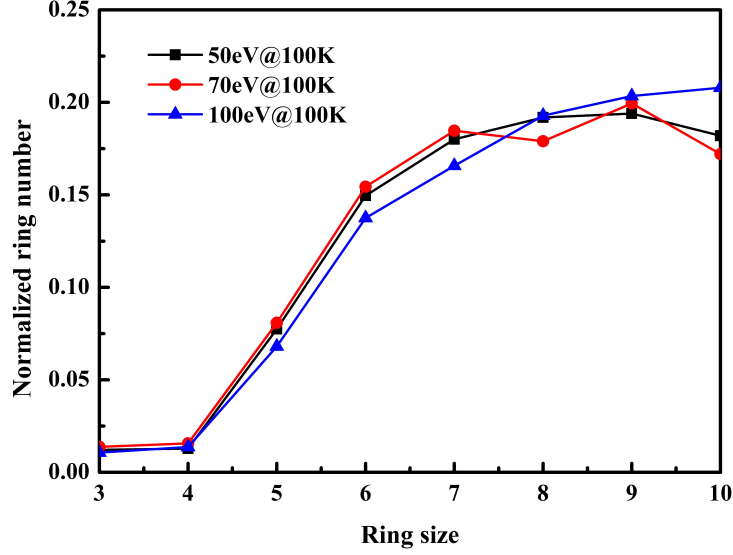


Figure 4: Normalized ring number as a function of ring size at 100 K under 50, 70, and 100 eV, respectively.

248 the more successful films with the larger quantity of the sp^3 atoms, while
 249 the film grown with the 100 eV incident energy exhibits the presence of the
 250 primitive rings with the higher number of ten-member rings, which indicates
 251 the reduction of structural quality of the film. Compared to the structure of
 252 the disordered amorphous carbon rather than graphite indicating that they
 253 are quite disordered since the six-element ring represents the structure more
 254 close to diamond and is the perfect primitive ring structure. This could be
 255 attributed to the relatively low sp^3 fraction in Table 1 compared to Ref. [35].
 256 Even so, DLC generated under 100 eV shows more disordered structure than
 257 that under 50 and 70 eV due to the relatively low fraction of six-element rings
 258 and high fraction of ten-element rings, meaning that 100 eV produced poorer
 259 quality of DLC comparing to other two energies when considering previous
 260 data and analysis. DLC deposited under 70 eV is only less disordered in
 261 a tiny degree than that under 50 eV comparing the six- and other-element
 262 rings. Hence, considering the sp^3 fraction, mass density, and disorder degree,
 263 we can draw the conclusion that 70 eV incident energy will lead to better
 264 quality of DLC deposited by carbon atoms continuously implanting.

265 3.3. Dangling bonds

266 The quality of DLC film is defined not only by the high sp^3 fraction and
 267 mass density, but also by the strength of adhesion of the film to the graphene
 268 top layer. Loose adhesion of the film to the substrate may result in sliding
 269 of the film along the graphene surface under external force. Since the C-
 270 C covalent bonds are strong and stable, the atoms with less neighbors than
 271 three at least will weaken the adhesion ability of the film in general. In Figure
 272 5 we plot the number of atoms with dangling bonds (< 3 neighbors) as a
 273 function of the z -coordinate. We also observe clear peaks at the positions
 274 corresponding to the interfaces between diamond and graphene, graphene
 275 and DLC, and at the open surface of DLC film. Unsaturated dangling bonds
 276 increase the energy of the interface reducing the barrier needed to detach the
 277 DLC film from the graphene surface.

278 Since we are interested in the interface between graphene and DLC, in this
 279 study we focus on the second peak from the left in Figure 5. Different symbols
 280 in the same plot show the results obtained at 100 K with different incident en-
 281 ergies. In Figure 5, there are slightly less atoms with dangling bonds created
 282 by ions with 100 eV than with 70 eV and the largest number of the dangling
 283 bonds is observed for the lowest incident energy. This clearly indicates that
 284 the high incident energy decreases the number of dangling bonds due to more
 285 intensive displacement cascades and activated atoms, which helps energetic
 286 atoms at the interface form bonds with others. The analysis of the content
 287 of dangling bonds in the graphene-DLC interface shows a clear competition
 288 between the thermal and radiation-induced processes. In this study, ambient
 289 temperature (100 K) is quite low. Therefore, the thermal velocities are very
 290 small and the atoms do not have opportunity to saturate the dangling bonds
 291 without additional energy introduced by an impacting ion.

292 Based on this analysis, we conclude that the quality of film adhesion to
 293 multilayer graphene increases with increasing incident energy that counter-
 294 balanced by the poorer quality of the grown film structure at high energy.
 295 This is why, it is important to optimize the film growth condition by care-
 296 fully selecting the energy of carbon ions during the deposition of the film.
 297 Since the peaks for the dangling bonds at this interface created by 70 and
 298 100 eV are almost the same, we conclude that the ions with 70 eV transfer
 299 the optimal amount of energy to the lattice atoms to maximize the effect of
 300 bond saturation and protect more beneath graphene layers. At lower energy,
 301 the transferred energy may not be sufficient and at higher energy induces too

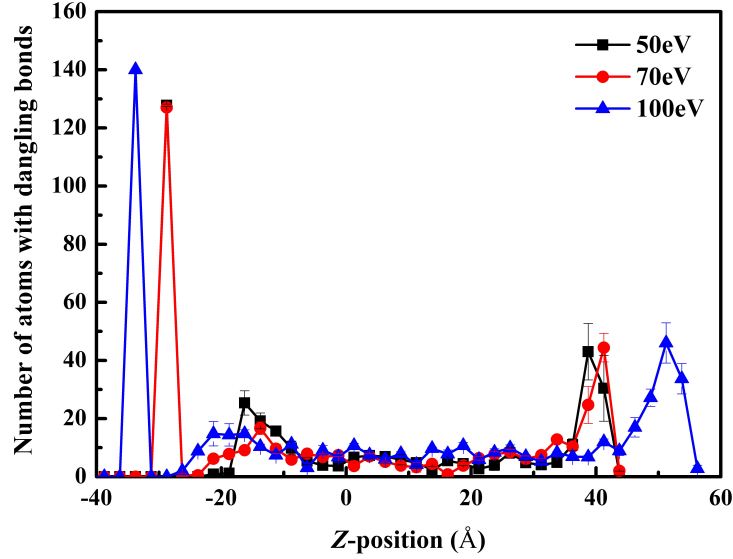


Figure 5: Number of atoms with dangling bonds as a function of z-position under different incident energies at 100 K. Each data point is averaged on the last frame of last 10 incidents and with error bars representing standard deviation.

strong movement of atoms that the bonds remain dangling and also graphene layers are consumed (see the remaining intact graphene layers).

4. Conclusions

In this study, we analyzed the quality of the DLC films deposited on multilayer graphene as a protective layer with different energy of incident carbon ions. We showed that in spite of sp^2 -bonding of carbon atoms in graphene, which impedes the formation of sp^3 -hybridization, DLC film can grow above graphene by careful selection of optimal deposition condition. We saw that sp^3 hybridization tends to appear in the middle part of DLC along z-direction due to the pressure induced transformation from sp^2 to sp^3 hybridization. Deposition at 70 eV resulted in most fraction of sp^3 -bonded atoms and the highest mass density. They dropped with both increasing and decreasing incident energies. In the films, the sp^2 -bond length was very close on average to that of graphene, while the sp^3 -bond length was slightly longer than that in diamond. Clearly the atomic volume occupied by the sp^2 -bonded atoms was much larger than that of sp^3 -bonded atoms, but yet, much smaller than in multilayer graphene. By analyzing the primitive rings in the

grown structures, we also concluded that the DLC grows above graphene is mainly disordered structure with a small amount of stable five and six-member rings. At the same time, the quality of the film adhesion improved with increase of incident energy at 100 K. The best adhesion was achieved with the energy of 100 eV. After comprehensive consideration of various situations, we concluded that 70 eV incident energy can provide best quality of DLC film while it can also retain good adhesion ability with graphene layers.

Acknowledgements

The sponsorship of Open Fund of Key Laboratory of Materials Preparation and Protection for Harsh Environment (Nanjing University of Aeronautics and Astronautics), Ministry of Industry and Information Technology (No. 56XCA18159-2) is gratefully acknowledged. This work is also supported by the Fundamental Research Funds for the Central Universities (Grant No. NJ20150021 and No. NJ20170012), the Funding of Jiangsu Innovation Program for Graduate Education (Grant No. KYLX15_0306) and the Fundamental Research Funds for the Central Universities. The support provided by China Scholarship Council (CSC) during a visit of Jian Liu to University of Helsinki is acknowledged as well.

References

- [1] H. Murayama, S. Tomonoh, J. M. Alford, M. E. Karpuk, Fullerene production in tons and more: from science to industry, Fuller. Nanotub. Car. N. 12 (2005) 1–9.
- [2] R. H. Baughman, A. A. Zakhidov, W. A. De Heer, Carbon nanotubes—the route toward applications, Science 297 (2002) 787–792.
- [3] H. Huang, X. Tang, F. Chen, J. Liu, H. Li, D. Chen, Graphene damage effects on radiation-resistance and configuration of copper–graphene nanocomposite under irradiation: A molecular dynamics study, Sci. Rep. 6 (2016) 39391.
- [4] V. B. Mohan, H. Souri, K. Jayaraman, D. Bhattacharyya, Mechanical properties of thin films of graphene materials: A study on their structural quality and functionalities, Curr. Appl. Phys. 18 (2018) 879–885.

- [5] H. Sun, C. Fu, Y. Gao, P. Guo, C. Wang, W. Yang, Q. Wang, C. Zhang, J. Wang, J. Xu, Electrical property of macroscopic graphene composite fibers prepared by chemical vapor deposition, *Nanotechnology* 29 (2018) 305601.
- [6] G. Qin, Z. Qin, H. Wang, M. Hu, On the diversity in the thermal transport properties of graphene: A first-principles-benchmark study testing different exchange-correlation functionals, *Comp. Mater. Sci.* 151 (2018) 153–159.
- [7] F. A. de Souza, R. G. Amorim, J. Prasongkit, W. L. Scopel, R. H. Scheicher, A. R. Rocha, Topological line defects in graphene for applications in gas sensing, *Carbon* 129 (2018) 803–808.
- [8] S. Dervin, D. D. Dionysiou, S. C. Pillai, 2d nanostructures for water purification: graphene and beyond, *Nanoscale* 8 (2016) 15115–15131.
- [9] U. Khan, T.-H. Kim, H. Ryu, W. Seung, S.-W. Kim, Graphene triboelectronics for electronic skin and touch screen applications, *Adv. Mater.* 29 (2017) 1603544.
- [10] M.-S. Lee, K. Lee, S.-Y. Kim, H. Lee, J. Park, K.-H. Choi, H.-K. Kim, D.-G. Kim, D.-Y. Lee, S. Nam, et al., High-performance, transparent, and stretchable electrodes using graphene–metal nanowire hybrid structures, *Nano Lett.* 13 (2013) 2814–2821.
- [11] X. Liu, J. Pu, L. Wang, Q. Xue, Novel dlc/ionic liquid/graphene nanocomposite coatings towards high-vacuum related space applications, *Journal of Materials Chemistry A* 1 (2013) 3797–3809.
- [12] E. J. Siochi, Graphene in the sky and beyond, *Nature nanotechnology* 9 (2014) 745.
- [13] J. Robertson, Properties of diamond-like carbon, *Surface and Coatings Technology* 50 (1992) 185–203.
- [14] A. Voevodin, M. Donley, J. Zabinski, Pulsed laser deposition of diamond-like carbon wear protective coatings: a review, *Surface and Coatings Technology* 92 (1997) 42–49.

- [15] C. Wei, J.-F. Yang, F.-C. Tai, The stress reduction effect by interlayer deposition or film thickness for diamond like carbon on rough surface, *Diam. Relat. Mater.* 19 (2010) 518–524.
- [16] Y. J. Won, H. Ki, Effect of film gradient profile on adhesion strength, residual stress and effective hardness of functionally graded diamond-like carbon films, *Appl. Surf. Sci.* 311 (2014) 775–779.
- [17] K. Ankit, A. Varade, N. Reddy, S. Dhan, M. Chellamalai, P. Krishna, N. Balashanmugam, Synthesis of high hardness, low cof diamond-like carbon using rf-pecvd at room temperature and evaluating its structure using electron microscopy, *Diam. Relat. Mater.* 80 (2017) 108–112.
- [18] N. Klyui, A. Liptuga, V. Lozinskii, A. Lukyanov, A. Oksanich, V. Terban, Application of diamond-like carbon films to increase transmission of semi-insulating gaas crystals in the ir spectral range, *Tech. Phys. Lett.* 38 (2012) 609–612.
- [19] K. Bewilogua, D. Hofmann, History of diamond-like carbon films—from first experiments to worldwide applications, *Surf. Coat. Tech.* 242 (2014) 214–225.
- [20] K. Ankit, A. Varade, N. Reddy, S. Dhan, M. Chellamalai, N. Balashanmugam, P. Krishna, Synthesis of high hardness ir optical coating using diamond-like carbon by pecvd at room temperature, *Diam. Relat. Mater.* 78 (2017) 39–43.
- [21] P. R. Goglia, J. Berkowitz, J. Hoehn, A. Xidis, L. Stover, Diamond-like carbon applications in high density hard disc recording heads, *Diam. Relat. Mater.* 10 (2001) 271–277.
- [22] A. Grill, Diamond-like carbon coatings as biocompatible materials—an overview, *Diam. Relat. Mater.* 12 (2003) 166–170.
- [23] L. Bai, G. Zhang, Z. Lu, Z. Wu, Y. Wang, L. Wang, P. Yan, Tribological mechanism of hydrogenated amorphous carbon film against pairs: a physical description, *J. Appl. Phys.* 110 (2011) 033521.
- [24] C. Donnet, A. Erdemir, Historical developments and new trends in tribological and solid lubricant coatings, *Surf. Coat. Tech.* 180 (2004) 76–84.

- 413 [25] W. L. Shi, X. T. Wei, W. Zhang, Z. G. Wang, C. H. Dong, S. Li,
414 Developments and applications of diamond-like carbon, in: Appl. Mech.
415 Mater., volume 864, Trans Tech Publ, pp. 14–24.
- 416 [26] H. Schittenhelm, D. B. Geohegan, G. Jellison, A. A. Puretzky, M. J.
417 Lance, P. F. Britt, Synthesis and characterization of single-wall carbon
418 nanotube–amorphous diamond thin-film composites, Appl. Phys. Lett.
419 81 (2002) 2097–2099.
- 420 [27] H. Kinoshita, I. Ippei, H. Sakai, N. Ohmae, Synthesis and mechani-
421 cal properties of carbon nanotube/diamond-like carbon composite films,
422 Diam. Relat. Mater. 16 (2007) 1940–1944.
- 423 [28] A. H. Lettington, Applications of diamond-like carbon thin films, Car-
424 bon 36 (1998) 555–560.
- 425 [29] D. Varshney, B. R. Weiner, G. Morell, Growth and field emission study
426 of a monolithic carbon nanotube/diamond composite, Carbon 48 (2010)
427 3353–3358.
- 428 [30] N. Sakudo, N. Ikenaga, H. Yasui, K. Awazu, Amorphous carbon coating
429 mixed with nano-diamonds, Thin Solid Films 516 (2008) 4483–4486.
- 430 [31] J. Zhang, Y. Yu, D. Huang, Good electrical and mechanical proper-
431 ties induced by the multilayer graphene oxide sheets incorporated to
432 amorphous carbon films, Solid State Sci. 12 (2010) 1183–1187.
- 433 [32] J. Baimova, L. K. Rysaeva, A. Rudskoy, Deformation behavior of
434 diamond-like phases: Molecular dynamics simulation, Diam. Relat.
435 Mater. 81 (2018) 154–160.
- 436 [33] Y. Wang, J. Xu, Y. Ootani, S. Bai, Y. Higuchi, N. Ozawa, K. Adachi,
437 J. M. Martin, M. Kubo, Tight-binding quantum chemical molecular
438 dynamics study on the friction and wear processes of diamond-like car-
439 bon coatings: Effect of tensile stress, ACS Appl. Mater. Inter. 9 (2017)
440 34396–34404.
- 441 [34] Y. Wang, J. Xu, J. Zhang, Q. Chen, Y. Ootani, Y. Higuchi, N. Ozawa,
442 J. M. Martin, K. Adachi, M. Kubo, Tribochemical reactions and graphi-
443 tization of diamond-like carbon against alumina give volcano-type tem-
444 perature dependence of friction coefficients: A tight-binding quantum
445 chemical molecular dynamics simulation, Carbon 133 (2018) 350–357.

- 446 [35] W. Ren, A. Iyer, J. Koskinen, A. Kaskela, E. I. Kauppinen, K. Avcha-
 447 ciov, K. Nordlund, Conditions for forming composite carbon nanotube-
 448 diamond like carbon material that retain the good properties of both
 449 materials, J. Appl. Phys. 118 (2015) 194306.
- 450 [36] D. McKenzie, Tetrahedral bonding in amorphous carbon, Rep. Prog.
 451 Phys. 59 (1996) 1611.
- 452 [37] J. Robertson, Diamond-like amorphous carbon, Mater. Sci. Eng. R 37
 453 (2002) 129–281.
- 454 [38] K. Nordlund, M. Ghaly, R. Averback, M. Caturla, T. D. de La Rubia,
 455 J. Tarus, Defect production in collision cascades in elemental semicon-
 456 ductors and fcc metals, Phys. Rev. B 57 (1998) 7556.
- 457 [39] M. Ghaly, K. Nordlund, R. Averback, Molecular dynamics investiga-
 458 tions of surface damage produced by kiloelectronvolt self-bombardment
 459 of solids, Philos. Mag. A 79 (1999) 795–820.
- 460 [40] D. W. Brenner, Empirical potential for hydrocarbons for use in simu-
 461 lating the chemical vapor deposition of diamond films, Phys. Rev. B 42
 462 (1990) 9458.
- 463 [41] D. W. Brenner, Erratum: Empirical potential for hydrocarbons for use
 464 in simulating the chemical vapor deposition of diamond films, Phys.
 465 Rev. B 46 (1992) 1948.
- 466 [42] K. Beardmore, R. Smith, Empirical potentials for c-si-h systems with
 467 application to c60 interactions with si crystal surfaces, Philos. Mag. A
 468 74 (1996) 1439–1466.
- 469 [43] H. Jäger, K. Albe, Molecular-dynamics simulations of steady-state
 470 growth of ion-deposited tetrahedral amorphous carbon films, J. Appl.
 471 Phys. 88 (2000) 1129–1135.
- 472 [44] N. Marks, Modelling diamond-like carbon with the environment-
 473 dependent interaction potential, Journal of Physics: Condensed Matter
 474 14 (2002) 2901.
- 475 [45] A. Stukowski, Visualization and analysis of atomistic simulation data
 476 with ovito—the open visualization tool, Model. Simul. Mater. Sc. 18
 477 (2009) 015012.

- 478 [46] H. J. Berendsen, J. v. Postma, W. F. van Gunsteren, A. DiNola, J. Haak,
479 Molecular dynamics with coupling to an external bath, *J. Chem. Phys.*
480 81 (1984) 3684–3690.
- 481 [47] X. Yuan, A. Cormack, Efficient algorithm for primitive ring statistics
482 in topological networks, *Comp. Mater. Sci.* 24 (2002) 343–360.
- 483 [48] J. Liu, X. Tang, Y. Li, Z. Dai, F. Chen, H. Huang, H. Li, H. Liu,
484 D. Chen, Effects of irradiation-induced structure evolution on the adhe-
485 sion force and instantaneous modulus of multi-walled carbon nanotube
486 arrays, *Mater. Chem. Phys.* 196 (2017) 160–169.
- 487 [49] J. Tersoff, Empirical interatomic potential for carbon, with applications
488 to amorphous carbon, *Phys. Rev. Lett.* 61 (1988) 2879.
- 489 [50] A. A. Zavitsas, The relation between bond lengths and dissociation
490 energies of carbon- carbon bonds, *The Journal of Physical Chemistry*
491 A 107 (2003) 897–898.